Three-dimensional mapping of optical near field of a nanoscale bowtie antenna

Rui Guo*, Edward C. Kinzel, Yan Li, Sreemanth M. Uppuluri, Arvind Raman, and Xianfan Xu

School of Mechanical Engineering and Birck Nanotechnology Center, Purdue University, West Lafayette, IN 47907,USA

**guoruikd@gmail.com*

Abstract: Ridge nanoscale aperture antennas have been shown to be a high transmission nanoscale light source. They provide a small, polarization-dependent near-field optical spot with much higher transmission efficiency than circularly-shaped apertures with similar field confinement. This provides significant motivations to understand the electromagnetic fields in the immediate proximity to the apertures. This paper describes an experimental three-dimensional optical near-field mapping of a bowtie nano-aperture. The measurements are performed using a home-built near-field scanning optical microscopy (NSOM) system. An aluminum coated Si_3N_4 probe with a 150 nm hole at the tip is used to collect optical signals. Both contact and constant-height scan (CHS) modes are used to measure the optical intensity at different longitudinal distances. A force-displacement curve is used to determine the tip-sample separation distance allowing the optical intensities to be mapped at distances as small as 50 nm and up to micrometer level. The experimental results also demonstrate the polarization dependence of the transmission through the bowtie aperture. Numerical simulations are also performed to compute the aperture's electromagnetic near-field distribution and are shown to agree with the experimental results.

OCIS codes: (180.4243) Near-field microscopy; (310.6628) Subwavelength structures, nanostructures.

References and links

1. Z. Rao, L. Hesselink, and J. S. Harris, "High transmission through ridge nano-apertures on Vertical-Cavity Surface-Emitting Lasers," Opt. Express **15**(16), 10427–10438 (2007).
2. A. Sundaramurthy, P. J. Schuck, N. R. Conley, D. P. Fromm, G. S. Kino, and W. E. Moerner, "Toward nanometer-scale optical photolithography: utilizing the near-field of bowtie optical nanoantennas," Nano Lett. **6**(3), 355–360 (2006).
3. E. Jin, and X. Xu, "Obtaining subwavelength optical spots using nanoscale ridge apertures," J. Heat Transfer **129**(1), 37 (2007).
4. L. Wang, S. M. Uppuluri, E. X. Jin, and X. Xu, "Nanolithography using high transmission nanoscale bowtie apertures," Nano Lett. **6**(3), 361–364 (2006).
5. K. Sendur, W. Challener, and C. Peng, "Ridge waveguide as a near field aperture for high density data storage," J. Appl. Phys. **96**(5), 2743 (2004).
6. S. Park, and J. Won Hahn, "Plasmonic data storage medium with metallic nano-aperture array embedded in dielectric material," Opt. Express **17**(22), 20203–20210 (2009).
7. A. Kinkhabwala, Z. Yu, S. Fan, Y. Avlasevich, K. Müllen, and W. Moerner, "Large single-molecule fluorescence enhancements produced by a bowtie nanoantenna," Nature Photonics **3**, 654–657 (2009).
8. E. Jin, and X. Xu, "Enhanced optical near field from a bowtie aperture," Appl. Phys. Lett. **88**(15), 153110 (2006).
9. L. Zhou, Q. Gan, F. J. Bartoli, and V. Dierolf, "Direct near-field optical imaging of UV bowtie nanoantennas," Opt. Express **17**(22), 20301–20306 (2009).
10. E. Lee, and J. Hahn, "Modeling of three-dimensional photoresist profiles exposed by localized fields of high-transmission nano-apertures," Nanotechnology **19**(27), 275303 (2008).
11. L. Wang, and X. Xu, "Numerical study of optical nanolithography using nanoscale bow-tie-shaped nano-apertures," J. Microsc. **229**(Pt 3), 483–489 (2008).

#122970 - $15.00 USD Received 19 Jan 2010; revised 14 Feb 2010; accepted 17 Feb 2010; published 24 Feb 2010

12. E. Betzig, P. Finn, and J. Weiner, "Combined shear force and near field scanning optical microscopy," Appl. Phys. Lett. **60**(20), 2484 (1992).
13. R. Toledo-Crow, P. Yang, Y. Chen, and M. Vaez Iravani, "Near field differential scanning optical microscope with atomic force regulation," Appl. Phys. Lett. **60**(24), 2957 (1992).
14. K. Karrai, and R. Grober, "Piezoelectric tip sample distance control for near field optical microscopes," Appl. Phys. Lett. **66**(14), 1842 (1995).
15. D. Tsai, and Y. Lu, "Tapping-mode tuning fork force sensing for near-field scanning optical microscopy," Appl. Phys. Lett. **73**(19), 2724 (1998).
16. B. Hecht, H. Bielefeldt, Y. Inouye, D. Pohl, and L. Novotny, "Facts and artifacts in near-field optical microscopy," J. Appl. Phys. **81**(6), 2492 (1997).
17. C. Jordan, S. Stranick, L. Richter, and R. Cavanagh, "Removing optical artifacts in near-field scanning optical microscopy by using a three-dimensional scanning mode," J. Appl. Phys. **86**(5), 2785 (1999).
18. L. Aigouy, Y. De Wilde, and M. Mortier, "Local optical imaging of nanoholes using a single fluorescent rare-earth-doped glass particle as a probe," Appl. Phys. Lett. **83**(1), 147–149 (2003).
19. L. Aigouy, P. Lalanne, J. P. Hugonin, G. Julié, V. Mathet, and M. Mortier, "Near-field analysis of surface waves launched at nanoslit apertures," Phys. Rev. Lett. **98**(15), 153902 (2007).
20. B. Gady, D. Schleef, R. Reifenberger, and D. S. Rimai, "The Interaction between Micrometer-size Particles and Flat Substrates: A Quantitative Study of Jump-to-Contact," J. Adhes. **67**(1), 291–305 (1998).
21. L. Verslegers, P. B. Catrysse, Z. Yu, J. S. White, E. S. Barnard, M. L. Brongersma, and S. Fan, "Planar lenses based on nanoscale slit arrays in a metallic film," Nano Lett. **9**(1), 235–238 (2009).
22. L. Wang, and X. Xu, "High transmission nanoscale bowtie-shaped aperture probe for near-field optical imaging," Appl. Phys. Lett. **90**(26), 261105 (2007).

1. Introduction

Nanoscale apertures are key elements for near-field optical engineering applications. They can provide a light source that is not diffraction limited. However, circular or square apertures with dimensions much smaller than the wavelength of light suffer from very low transmission. Changing the aperture shape has been shown to dramatically improve their efficiency. One example is nanoscale ridge aperture antennas [1,2]. A bowtie-shaped aperture can produce a narrow peak intensity distribution with a FWHM (full-width at half maximum) of tens of nanometers, and its peak intensity can be orders of magnitude higher than a circularly-shaped aperture with a similar level of field confinement [3].

Bowtie ridge antennas have been used to provide focused spots for many applications including nanoscale lithography fabrication [4], data storage [5,6], and single-molecule fluorescence measurement [7]. Accurate measurements of the near-field optical intensity distribution of these nano-apertures are important. A commonly used tool for such measurements is near-field scanning optical microscopy (NSOM). Since the demonstration in 1984, NSOM has become an important tool for sub-wavelength resolution optical measurement. Jin et al. measured the two-dimensional near-field intensity of a bowtie nano-aperture [8]. Zhou et. al used NSOM to determine the relationship of antenna size and optical field enhancement [9]. Lee et al. [10] obtained a three-dimensional optical distribution by measuring photoresist profiles exposed by the localized fields of bowtie nano-apertures at different gap distances. However, to the best of the authors' knowledge, the full three-dimensional near-field optical distribution as a function of the longitudinal direction using NSOM has not been reported. According to numerical studies [11] on bowtie ridge nano-aperture optical performance, the focused spot is a near-field source which decays exponentially within the distance of wavelength. Three-dimensional measurements are important to quantify the structure's optical performance and for applications in which the bowtie aperture and the sample are not in direct contact.

In a conventional illumination-collection NSOM system, a nanoscale aperture at the probe tip is used to collect near-field signal. A two-dimensional image is obtained by scanning the probe tip over the sample surface. In order to achieve three-dimensional near-field optical measurement, the tip-sample distance needs to be controlled. There are several ways to control the tip-sample distance in an NSOM system. One widely used method is to control the distance based on feedback of tip-sample force. For example, oscillating the tip laterally to the sample surface can be used to detect the damping produced by shear forces between the NSOM tip and the sample [12,13]. Similar techniques, such as tuning forks with sharp tips [14,15] and micro-cantilevers with optical detection feedback have also been used in

#122970 - $15.00 USD Received 19 Jan 2010; revised 14 Feb 2010; accepted 17 Feb 2010; published 24 Feb 2010

conjunction with closed-loop control. These dynamic methods are restricted to a range of tens of nanometers from the surface because the forces used for feedback are fundamentally short-range. Another widely used method is the constant-height scan (CHS) [16,17], which is a simpler method for three-dimensional optical near-field measurement. Aigouy et al. developed a single fluorescent rare-earth-doped glass particle-assisted NSOM and measured the three-dimensional local light intensities from nanoholes [18] and nanoslits [19] by using CHS. The CHS method permits the tip-sample distance to be specified from tens of nanometers to the micrometer range at which point the tip-sample interaction forces are negligible. During scanning, the tip-sample distance feedback is turned off, which makes it difficult to accurately control the tip-sample distance. This is especially true when the separation is less than 100 nm because the attractive force between probe and sample can make them jump to contact with each other. The jump-to-contact distance depends on several parameters such as tip-sample surface energies, Hamaker constants. as well as environmental factors [20].

In this paper, experimental results for the three-dimensional near-field optical and polarization-dependent measurement of bowtie nano-aperture are presented. We employ contact and CHS mode NSOM to investigate the three-dimensional near-field optical transmission from of a bowtie nano-aperture. Bowtie optical distribution measurements at the heights of 50 nm and up to micrometer level are achieved by carefully controlling sample surface quality, probe tip topography, as well as scanning parameters. The response of the bowtie nano-aperture is shown sensitive to the incident light polarization. Numerical studies have shown that when incident light is polarized across the two tips of the bowtie, a well confined near-field spot with high intensity is produced, however, the orthogonal polarization produces a poor field confinement [3]. We compare our experimental results to finite-element method (FEM) simulations of the near-field performance of the apertures. These are found to be in good agreement.

2. Experimental Setup and Sample Preparation

Figure 1 shows the schematic of our home-made illumination-collection mode NSOM setup. It is based on a typical Atomic Force Microscopy (AFM) feedback control system. The sample is placed on a three-dimensional piezoelectric stage (100 μm × 100 μm × 10 μm travel range) and illuminated by a linear-polarized, focused argon-ion laser (λ = 457 nm). A half-wave plate and a polarizer are used to control the polarization of the incident laser beam. Because the light source is fixed with respect to the NSOM tip instead of the sample, it is important to ensure the nano-aperture is uniform illuminated. In this experiment, the focused Gaussian illumination spot size is around 5 - 10μm by using a Nikon 5 × objective. Over the 260 nm by 260 nm bowtie aperture, the illumination intensity varies around 0.1%. The illumination distribution would need to be considered in order to measure larger samples. One solution would be to fabricate the structure to be studied on a laser diode which could be scanned relative to the probe [21].

#122970 - $15.00 USD Received 19 Jan 2010; revised 14 Feb 2010; accepted 17 Feb 2010; published 24 Feb 2010

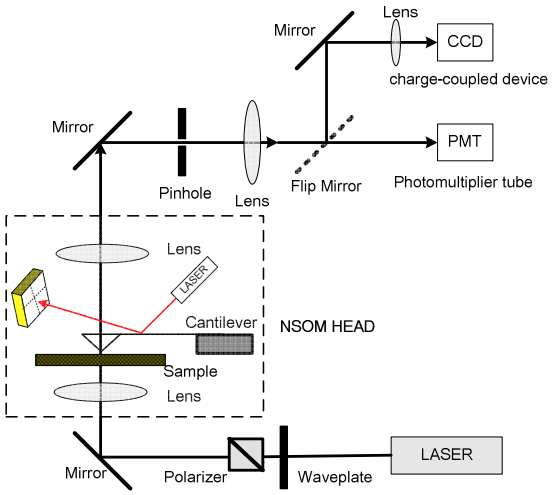

Fig. 1. Schematic of home-made NSOM system. The illumination source is a λ = 457 nm argon-ion laser. The feedback of NSOM head is based on the optical beam deflection technique. The NSOM probe is an aluminum coated Si_3N_4 probe with a 150 nm hole at the tip. The pinhole has a size of 100 micron.

The bowtie aperture is milled using a focused ion beam (FIB) machine into a 150 nm thick aluminum film evaporated onto an optically flat quartz substrate (flatness <λ/10). The aperture has outline dimensions of 260 × 260 nm and a gap of 62 nm as shown in Fig. 2(A). Light transmitted through the bowtie apertures is collected by a specially-fabricated NSOM probe with a hole of about 150 nm diameter at its tip [shown in Fig. 2(B)]. The probe is a Veeco Si_3N_4 probe. It was coated with a 100 nm thick aluminum film on the front side prior to FIB milling the hole at its apex. The nominal stiffness of the probe cantilever is 0.58 N/m. A 50 × objective lens is used to collect photons from the probe tip. A 100 μm pinhole is used as spatial filter to select photons from the plane at probe tip, which are measured by a photomultiplier tube. A flip mirror permits the experiment to be monitored by a CCD camera. The AFM controller (RHK SPM100) provides typical closed-loop operation as well as manual scanning without the feedback. This system has been used to successfully measure the near-field optical intensity distribution of nano-aperture in contact mode while being controlled by the normal force feedback based on the optical beam deflection technique [22].

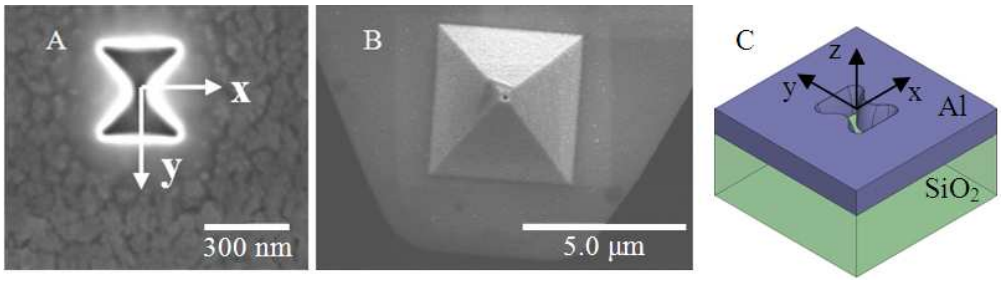

Fig. 2. (A) SEM image of the bowtie nano-aperture on a 150nm coated Al film. The aperture has a size of 260 nm × 260 nm and has a gap of 62 nm. (B) SEM image of the NSOM probe. The hole on the tip is around 150 nm in diameter. (C) Simulation model of bowtie nano-antenna. Its dimensions used in simulation are fit to SEM image (A).

Numerical simulations are performed using a commercial frequency domain finite-element method (FEM) package (HFSS from Ansoft LLC.) to calculate the near-field electromagnetic distribution of the bowtie aperture. The simulation model includes the 150 nm Al film on top of the fused silica substrate as shown in Fig. 2(C). The system is illuminated with a λ = 457

#122970 - $15.00 USD Received 19 Jan 2010; revised 14 Feb 2010; accepted 17 Feb 2010; published 24 Feb 2010

nm plane-wave. The aperture outline dimensions used in calculations are fit to the SEM images with the gap about 62 nm wide at the fused silica/aluminum interface and 134 nm at the top of the film. The calculated electric field distributions are shown in Fig. 3. Figures 3(A) and 3(B) show that when the incident light is x-polarized it is focused to a spot at the center of bowtie with two bright hot-spots at the tips. When the polarization is in the y-direction, the highest field intensities occur at the edges of the aperture as shown in Fig. 3(C) and less light overall passes through the center as shown in Fig. 3(D). A more detailed quantitative comparison of the experimental and simulation results will be given below.

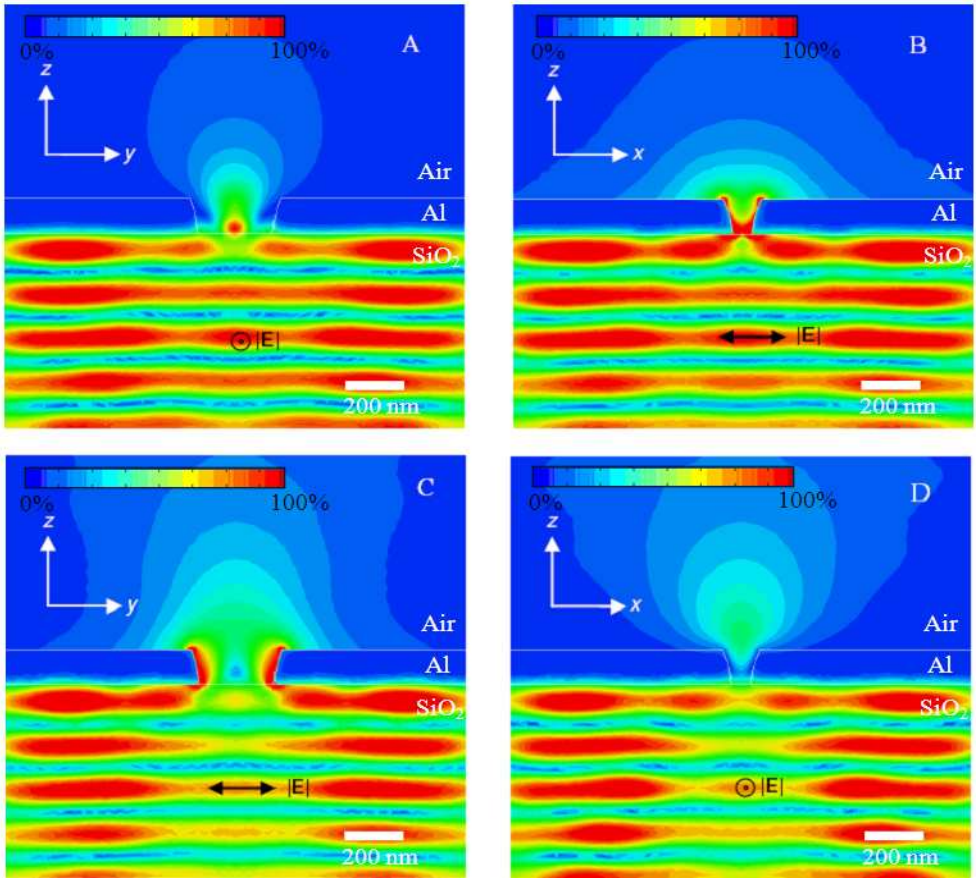

Fig. 3. Computed electric field distribution of bowtie aperture under x-polarized illumination (A, B) and y-polarized illumination (C, D). The aperture has a size of 260 nm × 260 nm and a gap of about 62 nm at the fused silica/aluminum interface and 134 nm at the top of the film. The illumination is a λ = 457 nm plane-wave.

3. Experimental results and discussions

In the contact mode, the NSOM probe is kept in contact with the sample surface using a closed-control loop to maintain a constant force (around 30 nN shown in Fig. 6) throughout the scanning process. This method works well to capture photons close to the surface sample. Figure 4(A) shows the near-field spot measured with contact mode scanning generated with the incident laser linearly polarized in the x-direction. There are 64 × 64 pixels in each image distributed over an area of 1 μm × 1 μm. The image was obtained with a scanning speed of 1.95 μm/s. Figure 4(B) shows the near-field spot measured in contact mode under y-polarized illumination. The two figures show the bowtie aperture's sensitivity to the polarization of the incident light. Both the spot shape and size are different with a circular and focused spot is

#122970 - $15.00 USD Received 19 Jan 2010; revised 14 Feb 2010; accepted 17 Feb 2010; published 24 Feb 2010

observed under x-polarized illumination. This spot has a FWHM of around 157 nm and peak intensity as high as 160 kHz in photon counts. For y-polarized illumination, multiple spots located at the corners of the bowtie aperture can be seen, while the peak intensity is lower (around 30 kHz). Considering a background noise level of 5 kHz, the peak intensity of the spot with y-polarized illumination is about 6.2 times weaker than that with x-polarized illumination.

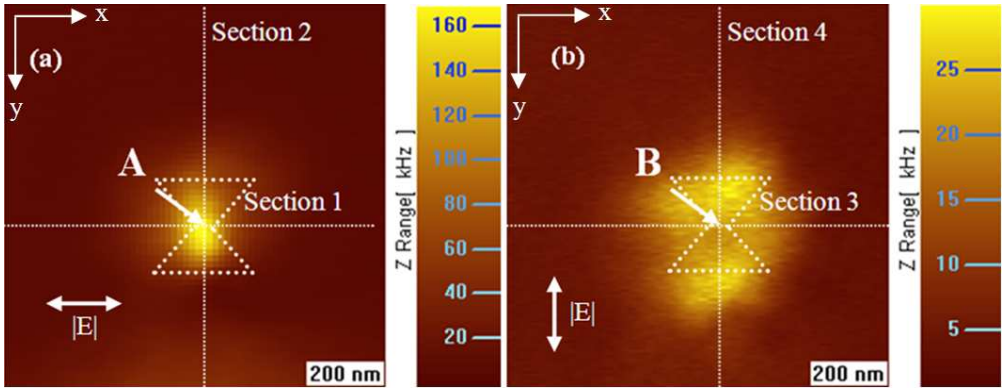

Fig. 4. Near-field intensity distribution of bowtie aperture measured in the contact mode. The scan area is 1μm × 1μm. The illumination laser is polarized along the x-direction (A) and y-direction (B). Note the different intensity scales in the two figures.

Three-dimensional mapping of the near-field intensity can be acquired by turning off the feedback and scanning the probe over the sample at a manually set height. This approach allows the measurement of the optical fields at submicron to micrometer tip-sample distances.

First, the tip-sample distance needs to be calibrated by measuring the force-displacement curve (F-z curve). Figure 5 shows the measured F-z curve by obtained when the NSOM probe approaches the sample surface directly above the bowtie center position "A", marked in Fig. 4(a). The optical signal is acquired simultaneously and shown in Fig. 5. At a certain distance from the surface, the probe snaps down into contact and the force change on the cantilever is detected. The tip-sample contact point is located at around −50 nm as shown in the abscissa of Fig. 5. This point (tip-sample contact position) is set as zero in the calibration of tip-sample distance. Figure 6 shows the optical data when the light polarized in the y-direction. In Fig. 5, the NSOM signal in the approaching direction (red line) has a peak of around 160 kHz located at the tip-sample contact position. When tip-sample distance is larger, especially when it is greater than 150 nm, the NSOM signal drops rapidly to less than 50 kHz. In Fig. 6, the NSOM signal has a peak number of around 30 kHz. As the tip-sample distance increases above 150 nm, the NSOM signal falls to 10 kHz. Figures 5 and 6 show that the light intensity decays quicker when the light is polarized in the x-direction than when it is polarized in the y-direction. When the tip-sample distance is larger than 200 nm, slight shifts in NSOM signal are found around −0.6 μm and −0.35 μm in the NSOM curve showed in Figs. 5 and 6. These are believed to result from Fabry-Perót electromagnetic interactions between NSOM cantilever/probe and sample. Some of the light emitted from the aperture reflected between Al coated cantilever and the Al bowtie sample surface to generate periodic interference when their separation changes. This interaction will slightly increase the background optical noise. In this work, we focus on near-field measurements in the range of 0 – 200 nm, where the interference is not constructive. The black and blue lines in Figs. 5 and 6 are F-z curve and NSOM signal, respectively, measured in retraction direction. After NSOM tip contacts with the sample surface, the retraction needs to overcome tip-sample attractive force (around −80nN in Fig. 5 and −140nN in Fig. 6). The force difference in Figs. 5 and 6 is likely caused by the worn-out NSOM tip. This attractive force will bend the NSOM cantilever and slightly shift the tip position, which results in the difference of NSOM signals collected at different directions in Figs. 5 and 6.

#122970 - $15.00 USD Received 19 Jan 2010; revised 14 Feb 2010; accepted 17 Feb 2010; published 24 Feb 2010

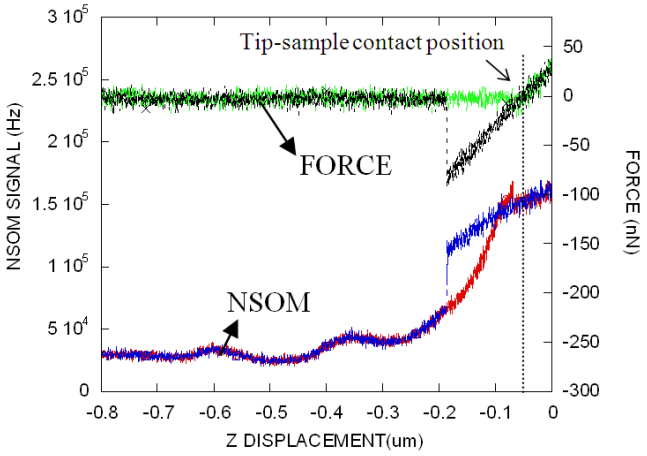

Fig. 5. NSOM signals and the F-z curve at the A position in Fig. 4(A). Data are collected at different directions. Tip approach direction: green and red; tip retraction direction: black and blue.

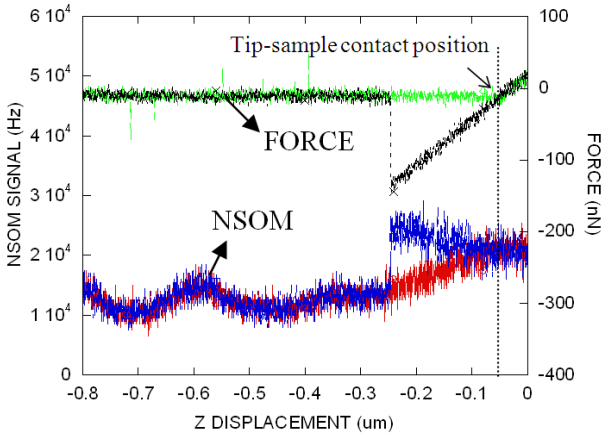

Fig. 6. NSOM signals and the F-z curve at the B position in Fig. 4(B). Data are collected at different directions. Tip approach direction: green and red; tip retraction direction: black and blue.

After calibration of the tip-sample distance using the F-z curve, a series of NSOM images are collected at different heights using CHS. As in contact, the images are collected over an area of 1 μm × 1 μm. There are 64 × 64 pixels in each image that are obtained with a scanning speed of 1.95 μm/s. During a CHS, the position of the probe is fixed, while the sample is located on a three-dimensional piezo-electric stage. The tip-sample distance is set by adjusting sample height shown as abscissa in Figs. 5 and 6. The tip-sample distances for CHS measurements are selected as 50 nm, 75 nm, 100 nm, 125 nm, 150 nm and 200 nm relative to the "tip-sample contact point" as zero as shown in Fig. 5. The optical images obtained at selected heights can be combined with the contact measurement to construct a three-dimensional map of the bowtie optical near-field distribution.

Figure 7 shows the images at six different heights, obtained under x-polarized illumination. In Fig. 7(A), a focused oval-shaped spot with a size of 213nm (x-direction) × 229nm (y-direction) can be recognized. According to theory, the electromagnetic fields from a nanoscale light source should decay with respect to distance exponentially. These images show that the light rapidly diverges away from the bowtie aperture and the peak intensity also decreases quickly. It is found that the spot almost disappears at 200nm-distance in Fig. 7(F) which agrees with near-field optical theory. Figure 8 shows near-field distributions of the

#122970 - $15.00 USD Received 19 Jan 2010; revised 14 Feb 2010; accepted 17 Feb 2010; published 24 Feb 2010

bowtie aperture when the polarization is in the y-direction. A multi-spot pattern can be recognized in Figs. 8(A) and 8(B). This multi-spot distribution locates at corners of the bowtie aperture which agrees with the simulation results shown in Fig. 3. It is found that the spot size is bigger than the outline dimension of bowtie aperture which is believed to be caused by the 150nm-diameter NSOM tip. As the tip-sample distance becomes greater, the multi-spot pattern disappears and peak intensity decreases from 30 kHz to a lower level around 10 kHz. The spot intensity in y-polarized illumination decays slower than x-polarization. It agrees with the simulation in Fig. 3.

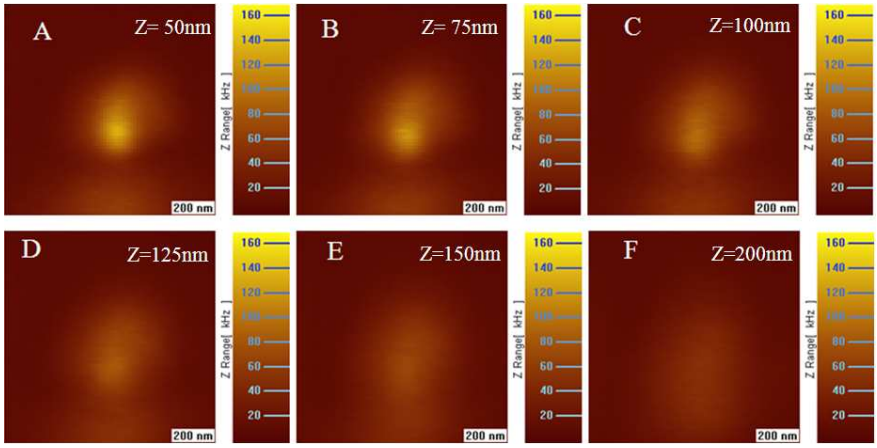

Fig. 7. Constant-height scanning NSOM images at difference tip-sample distances: 50 nm, 75 nm, 100 nm, 125 nm, 150 nm and 200 nm in A - F, respectively. The laser polarization is in the x-direction.

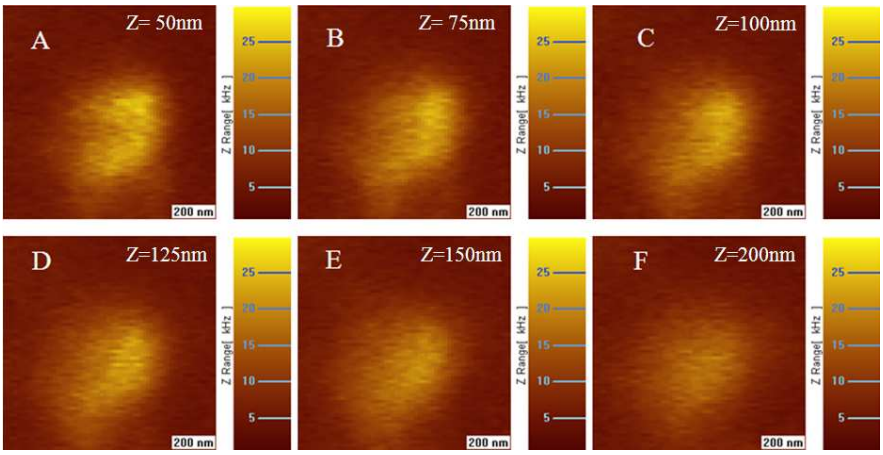

Fig. 8. Constant-height scanning NSOM images at different tip-sample distances: 50 nm, 75 nm, 100 nm, 125 nm, 150 nm and 200 nm in A - F, respectively. The laser polarization is in the y-direction.

In order to further understand the three-dimensional near-field optical distribution, their cross sections at different heights are plotted along with the corresponding simulation results. Figures 9(A) and (B) show NSOM signal and computed electric field of Section 1 of Fig. 4(A) at different tip-sample distances. For the 50 nm-distance curve in Fig. 9(A), the NSOM signal has a peak of 132 kHz. This number drops to 49 kHz in the 200 nm-distance curve (a factor of 2.7). In Fig. 9(B), the corresponding theoretical peak intensity at the distance of 50 nm is 0.76 V/m. This number changes to 0.27 V/m at the distance of 200 nm (a factor of about 2.8). In Fig. 9(B), the 50 nm-distance curve has two peaks at the positions x = 0.44 μm and 0.56 μm.

#122970 - $15.00 USD Received 19 Jan 2010; revised 14 Feb 2010; accepted 17 Feb 2010; published 24 Feb 2010

The two peaks come from the bowtie's two tips. The experimental results do not show the two peaks because the 150 nm-diameter aperture at the NSOM scanning tip is not small enough to resolve these two peaks. Figures 9(C) and 9(D) shows the NSOM signal and the computed electric field along Section 2 of Fig. 4(A) at different tip-sample distances. The peak intensity also drops rapidly when increasing tip-sample distance. In Fig. 9(C), an increase in the noise level could be found at the range of x = 0.8 μm to x = 1 μm. This increase is caused by light leaking around the edge of the NSOM cantilever. When NSOM tip is scanning over the bowtie sample, the photons from the passing through probe aperture are collected and counted by the PMT, while all the other photons coming from the bowtie are blocked by NSOM cantilever. The fact that the cantilever is much wider than the probe has a significant role for maintaining a low noise level in the measurement. During the data acquisition, the cantilever can scan over a region large enough so that the line of sight from the bowtie aperture to the PMT is not blocked by the cantilever. This introduces an additional small noise level change at different locations. When data is acquired in contact mode, the NSOM tip collects signals according to the topography of the sample surface. This changes the interrogation volume so that it does not necessarily correspond to the simulation data from the bowtie apertures exit plane (z = 0). The FWHM of the near-field spot size after Gaussian fits of Fig. 9 are shown in Table 1. When the tip-sample distance increases from contact to a distance of 200 nm, the FWHM of the optical signal in Fig. 9(A) increases about 1.9 times from 157 nm to 305 nm while the corresponding FWHM of simulated aperture response from Fig. 9(B) increases about 2.2 times from 246 nm to 539 nm. For Fig. 9(C), its FWHM increases from 169 nm to 499 nm (3.0 times) while the simulated data increases from 137 nm to 403 nm (2.9 times). The differences between the measured and calculated FWHM sizes are likely due to the differences in the dimensions of the bowtie geometries used in the calculations vs. in the experiments.

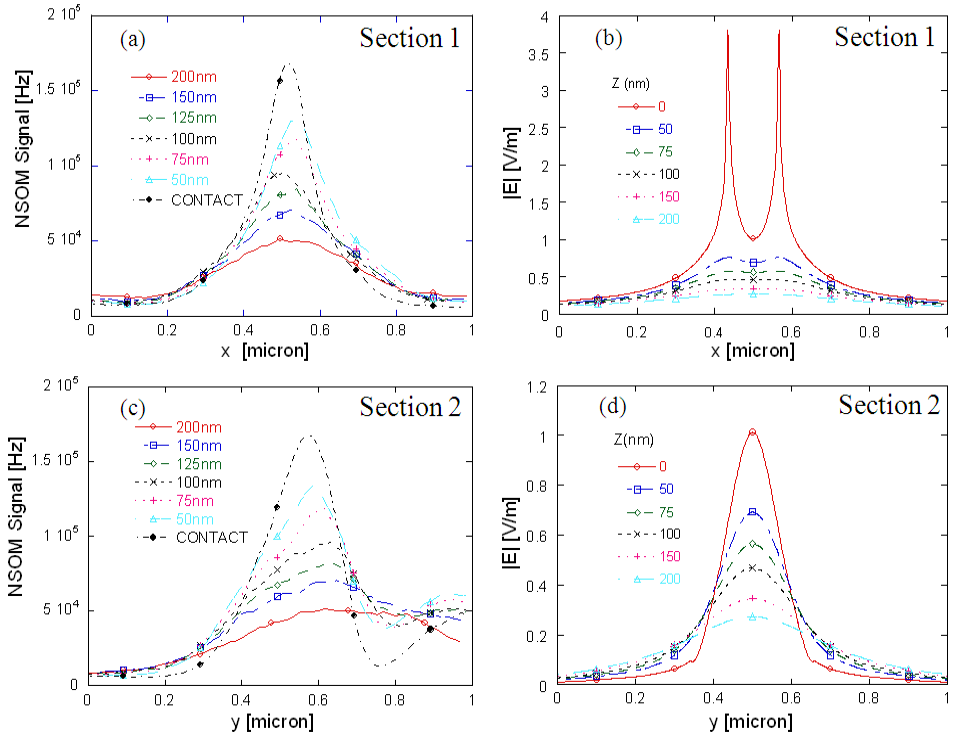

Fig. 9. Experimental (A,C) and theoretical (B,D) intensity distribution along sections 1 and 2 of Fig. 4(A), respectively, at different heights for laser polarization in the x-direction.

#122970 - $15.00 USD Received 19 Jan 2010; revised 14 Feb 2010; accepted 17 Feb 2010; published 24 Feb 2010

Table 1. Measured FWHM of near-field spot at different heights [a]

	X FWHM(nm)		Y FWHM(nm)	
Height(nm)	*Exp.*	*Sim.*	*Exp.*	*Sim.*
Contact/Z = 0	157	246	169	137
50	213	342	229	194
75	219	383	277	229
100	245	418	368[b]	266
150	292	481	433[b]	339
200	305	539	499[b]	403

[a] From Gaussian fits of Fig. 9.
[b] These Gaussian fits are done in the region of y = 0~0.8μm to reduce noise effect.

Figure 10 shows the theoretical and experimental near-field distributions at different tip-sample distances under y-polarized illumination. Figure 10(A) shows the NSOM signal along section 3 of Fig. 4(B) at different tip-sample distances. The peak signal in the 50 nm-distance curve is 23 kHz. As the tip-sample distance increases to 150 nm, there is little change of the peak intensity, which is 21 kHz. As the distance increases to 200 nm, the peak intensity drops slightly to 18 kHz. The total drop in the NSOM signal is about 15%. In Fig. 10(B), the corresponding calculated peak intensity at 50 nm is 0.76 V/m. The peak intensities for 75 nm, 100 nm, 150 nm and 200 nm are 0.75, 0.73, 0.64 and 0.56 V/m, respectively. The total drop from 50nm to 200nm is about 26%. Figure 10(C) shows NSOM signal of section 4 of Fig. 4(B) at different tip-sample distances from 50 nm to 200 nm. Similarly, the decrease of the peak intensity with the increasing tip-sample distance can be found from both experimental and simulation results. When the tip-sample distance increases from 50nm to 200 nm, the peak intensity of the optical signal in Fig. 10(C) decreases about 24% from 23 kHz to 17.5 kHz while the corresponding simulated response from Fig. 10(D) decreases about 44% from 1 to 0.56 V/m. Multi-peak shape is shown in contact, 50 nm, 75 nm and 100 nm curves in Fig. 10(C). The same patterns can be found in the corresponding curves in Fig. 10(D). For example, the 50 nm-distance curve in Fig. 10(C) has two peaks at the positions x = 0.49 μm and 0.74 μm. The two peaks have a separation of about 0.25 μm. In its simulated result of Fig. 10(D), the 50 nm-distance curve has two peaks at x = 0.38μm and 0.62μm with a separation of 0.24μm.

#122970 - $15.00 USD Received 19 Jan 2010; revised 14 Feb 2010; accepted 17 Feb 2010; published 24 Feb 2010

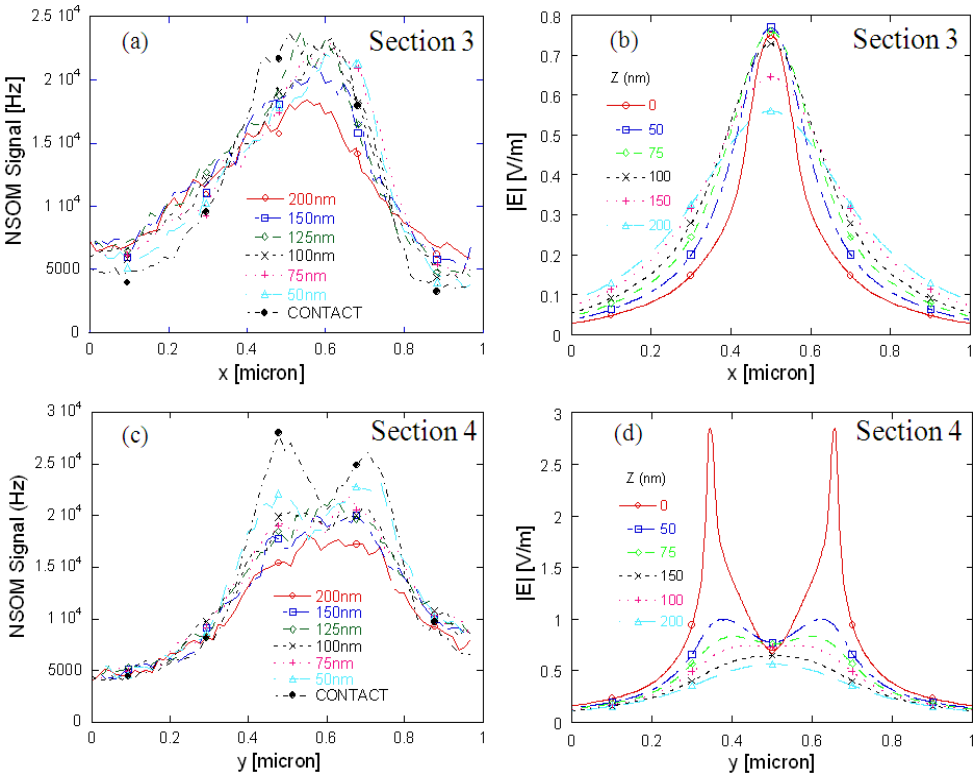

Fig. 10. Experimental (A,C) and theoretical (B,D) intensity distribution along sections 3 and 4 in Fig. 4(B), respectively, at different heights for laser polarization in the y-direction.

4. Conclusions

The three-dimensional near-field distribution from a nanoscale bowtie aperture antenna is measured. The experimental result shows that the near-field distribution is sensitive to polarization of incident light. When the light is polarized in the x-direction, a single focused spot is obtained with FWHM of 157 nm, the measurement of which is limited by the aperture size of the NSOM probe. The intensity of near-field decreases quickly within 200 nm. When the light is polarized in the y-direction, multiple spots are obtained, which are located at the edges of the bowtie aperture. These results are consistent with the numerical simulations of the near-field distributions of a bowtie antenna.

Acknowledgments

The financial support of this work by the National Science Foundation (NSF) grant 0707817 is acknowledged.

#122970 - $15.00 USD Received 19 Jan 2010; revised 14 Feb 2010; accepted 17 Feb 2010; published 24 Feb 2010